Applied Thermal Engineering 278 (2025) 127287

Contents lists available at ScienceDirect

Applied Thermal Engineering

journal homepage: www.elsevier.com/locate/apthermeng

Research Paper

Energy and exergy evaluation of R404A and R290 in a shelf-cooled commercial vertical deep freezer

Egemen Biçen, Seda Kırmacı Arabacı *

Mechanical Engineering Department, Manisa Celal Bayar University, Manisa, Turkey

ARTICLE INFO

Keywords:
Deep freezer
Exergy analysis
Energy efficiency
F-gas regulation
Carbon emissions

ABSTRACT

The European Union F-Gas regulation has accelerated the transition from high-GWP refrigerants to environmentally friendly alternatives in commercial vertical refrigeration systems. This study experimentally investigates the use of R290-propane as a replacement for R404A-hydrofluorocarbon in a shelf-cooled commercial vertical deep freezer without modifying external components. While previous studies primarily focused on energy analyses, this research uniquely integrates both energy and exergy evaluations. Experimental results show that the R290 system demonstrated a 7 % higher coefficient of performance and a 17 % increase in exergy efficiency compared to the R404A system, confirming its superior thermodynamic behavior. The total exergy losses in the R290 system were approximately 0.043 kW lower, primarily influenced by enhanced compressor performance, which contributed the most to system irreversibilities. Additionally, the system's equivalent carbon emissions were reduced by 99.92 %, highlighting its significant environmental advantages. These findings demonstrate that R290 is a highly efficient and sustainable alternative to R404A for commercial vertical refrigeration, offering improved thermodynamic performance, lower energy consumption, and a substantially reduced carbon footprint.

1. Introduction

The environmental impact of refrigerants with high Global Warming Potential (GWP), such as R404A, has become a major concern due to their contributions to climate change and ozone layer depletion. International frameworks like the Montreal Protocol and its amendments, alongside the Kyoto Protocol, have mandated the phase-out of ozone-depleting substances such as chlorofluorocarbons (CFCs) and hydrochlorofluorocarbons (HCFCs) [1–9]. Although hydrofluorocarbons (HFCs) were introduced as transitional replacements due to their zero Ozone Depletion Potential (ODP), their extremely high GWP—approximately 3921 for R404A—has prompted further regulatory restrictions [10,11]. The European Union's F-Gas Regulation [12] aims to reduce HFC consumption by 79 % by 2030, emphasizing the urgent need for environmentally friendly alternatives in commercial refrigeration sectors [13].

Among the proposed substitutes, R290 (propane) has gained increasing attention due to its excellent thermophysical properties, very low GWP (~3), and zero ODP [14–19,26,38]. Experimental investigations have confirmed that R290 not only improves the Coefficient of Performance (COP) but also reduces energy consumption when compared to R404A-based systems. For instance, Saraç and Ünaldı [20], Pektezel et al. [21], and Polukhin and Yakovleva [22] reported notable gains in COP and Energy Efficiency Ratio (EER) using R290 under comparable operating conditions. Similarly, Sethi et al. [23] evaluated R404A alternatives and highlighted R290-related blends as promising low-GWP candidates. Berkah Fajar et al. [24] experimentally retrofitted a vapor compression system with R290, achieving significant improvements in both energy and exergy performance indicators. A theoretical comparison by Koşan [25] further reinforced the thermodynamic suitability of R290 based on both energy and exergy criteria.

Despite its benefits, early adoption of R290 was limited by safety concerns related to its flammability. However, recent advancements in system architecture—such as compact and highly efficient heat exchangers that minimize refrigerant charge—and the implementation of rigorous safety standards have significantly mitigated these risks. These developments have enabled the broader adoption of R290 in commercial refrigeration systems, particularly in shelf-cooled vertical freezers [26–28].In parallel, studies have demonstrated that the amount of refrigerant charge plays a critical role in system efficiency. Optimizing charge levels not only improves thermal performance but also enhances

* Corresponding author.
E-mail address: seda.kirmaci@cbu.edu.tr (S.K. Arabacı).

https://doi.org/10.1016/j.applthermaleng.2025.127287
Received 10 February 2025; Received in revised form 14 May 2025; Accepted 20 June 2025
Available online 25 June 2025

Nomenclature

Abbreviation

ASHRAE	American Society of Heating, Refrigerating and Air-Conditioning Engineers
ACH	Air Change per Hour
CFCs	chlorofluorocarbons
COP	Coefficient of Performance
EnBE	Energy Balance Equation
EntBE	Entropy Balance Equation
ExBE	Exergy Balance Equation
EU	European Union
GWP	Global Warming Potential
HC	Hydro-Carbon
HFC	Hydro-Fluouro-Carbon
HCFC	Hydro-Chloro-Fluoro-Carbon
HFO	Hidro-Floro-Olefin
MBE	Mass Balance Equation
MTA	Medium temperature application
NBP	Normal boiling point (°C)
ODP	Ozone Depletion Potential

Symbols

$\dot{E}$	Energy rate (kW)
g	gravity acceleration (m-s^{-2})
h	specific enthalpy (kJ kg^{-1})
$\dot{m}$	mass flow rate (kg s^{-1})
P	pressure (kPa or bar)
$\dot{Q}$	heat transfer rate (kW)
s	specific entropy (kJ kg^{-1} K^{-1})
$\dot{S}$	entropy rate (kW K^{-1})
T	temperature (°C)
ΔT	temperature difference (–)
W	power (kW)
ex	specific exergy (kJ kg^{-1})
$\dot{E}$ x	exergy rate (kW)

Greek symbols

η	exergy efficiency (%)
ε	energy efficiency

Subscripts

cond	condenser
comp	compressor
CR	critical
dest	destruction
evap	evaporator
gen	generation
in	inlet
max	maximum
M	number of package
out	outlet
RSS	root-sum-square
SCCVDF	shelf-cooled commercial vertical deep freezer
TM,a	temperature of M−package (°C)

safety in hydrocarbon-based systems. For instance, Corberan et al. [29] and Cavallini et al. [31] showed that charge reduction through appropriate heat exchanger design can improve system reliability and performance. Fernando et al. [30] validated this experimentally in propane-based heat pumps, confirming efficient operation under reduced charge conditions. Additionally, Spatz and Motta [28] reported that R290 achieves favorable performance at lower volumetric flow rates compared to traditional refrigerants, further supporting its practical viability.

Despite the growing number of studies emphasizing R290′s energetic advantages, there remains a noticeable gap in the literature regarding its comprehensive exergy performance assessment. While energy analyses offer insights into system efficiency, exergy analyses are essential for identifying irreversibilities and pinpointing areas for optimization [25,32–37]. Only a limited number of studies have explored the exergy behavior of R290-based systems in commercial refrigeration applications.

A further gap exists in the context of advanced integrated systems. For example, Venegas et al. [41] highlighted the potential of liquid desiccant systems coupled with heat pumps to improve overall energy performance. However, these investigations primarily focus on system architecture and neglect refrigerant-level performance comparisons—particularly between R290 and conventional options like R404A. Thus, despite progress in component design and integration strategies, there is still a lack of targeted analysis evaluating the thermodynamic performance of low-GWP refrigerants in such systems.

In this context, recent experimental studies provide valuable insight. Saraç and Ünaldı [20] demonstrated that retrofitting a commercial vertical refrigeration system with R290 yielded substantial improvements in COP and energy efficiency. Similarly, Polukhin and Yakovleva [22] reported 38–44 % gains in Energy Efficiency Ratio (EER) and 26–31 % in COP compared to R404A under equivalent conditions. These findings reinforce the suitability of R290 as a drop-in replacement with minimal structural modification requirements.

Particularly in commercial vertical deep freezers—commonly used in retail environments—specific operational challenges arise. The presence of glass doors and frequent customer interactions result in significant warm air ingress, requiring both high cooling capacity and rapid temperature recovery to maintain food safety and product integrity [39]. These demanding conditions underline the importance of refrigerants that offer not only environmental advantages but also robust thermodynamic performance.

This study aims to contribute to sustainable refrigeration practices by experimentally investigating the energy and exergy performance of a shelf-cooled commercial vertical deep freezer retrofitted with R290. While most previous studies rely solely on energy evaluations, this work integrates exergy analysis to quantify system irreversibilities more accurately. Although R290 has been shown to enhance energy efficiency in various applications, comprehensive exergy assessments specifically for shelf-cooled commercial vertical deep freezers remain scarce in the literature. Accordingly, the present study evaluates the system's thermodynamic performance under realistic operating conditions using a holistic methodological framework.

2. Experimental procedure

A commercially available SCCVDF is experimentally investigated in this study. R290 is researched as a replacement for R404A in SCCVDF, which is the produce situation in the market, in order to comply with the EU F-gas Regulation. The original system designed for R404A refrigerant was retrofitted to operate with R290 by replacing the compressor, while keeping the cabinet structure, refrigerant lines, evaporator, and condenser unchanged. Investigated are the impacts of replacement on the SCCVDF's energetic and exergetic performance.

2.1. Description of investigated SCCVDF

SCCVDF is a type of deep freezer generally used in markets that

frozen foods are stored and displayed. SCCVDF has a glass door so that the products inside can be exhibited to the customer. The tested unit is a commercially available shelf-cooled vertical freezer designed for food display and storage in retail environments. The total volume of the freezer of SCCVDF is 370 L. The main figure of the SCCVDF and the general view of the test room are shown in Fig. 1. The external dimensions of SCCVDF are 640 mm (width) × 670 mm (depth) × 2056 mm (height). The operating temperature range is −18/−24 °C. The freezer compartment has an electronic thermostat to support energy saving by checking system fans among required temperature levels. The other compartments are Thermometer, LED Illumination and door handle.

A SCCVDF system operates heat transferring from a low temperature area to high temperature area, using a vapor compression cycle. The basic vapour compression cycle has of four parts; condenser, compressor, evaporator, and capillary tube are shown in Fig. 2.

SCCVDFs are deep freezers that are generally used in market stores where frozen foods are stored.

2.2. Refrigerant replacement

The existing study has been done with only compressor and refrigerant replacement without changing the geometry. Natural refrigerants are progressively used in MTAs. For deciding the best refrigerant for the applications, essential characteristics such as GWP, ODP etc. should be well-considered with the operating conditions. GWP values and ODP values, the physical properties of refrigerants, submitted to this research are given in Table 1. However, since it is in the R290 flammable class, it is in the A3 security class.

2.3. Instrumentation and measurements

The pressure measurements on the test setup are measured from the condenser outlet and the evaporator outlet as high and low pressure, respectively. Temperature measurements are taken from the pipe surface with thermocouples, and pressure measurements are measured by direct contact with the fluid with pressure transmitters. In the energy and exergy analyses, actual experimental measurements for compressor inlet and outlet conditions were used whenever available. These values were used to calculate the thermodynamic properties required for performance evaluation. Where direct measurements were not possible, outlet properties were estimated assuming isentropic compression adjusted by representative isentropic efficiency values. This approach ensures consistency between the theoretical assumptions and the experimental characteristics of the system. During the experiments, compressor power consumption and cooling capacity were measured, and the coefficient of performance (COP) was calculated accordingly. Two different compressors were used for the two refrigerants. The isentropic efficiencies of the compressors—0.51 for R404A and 0.55 for R290—were obtained from the technical datasheets provided by the manufacturer, Specifically, a compressor designed for R404A and another compatible with R290 were selected, based on their technical specifications and capacity ratings. These efficiencies were used to estimate theoretical mass flow rates and to validate the net electrical power consumption by excluding auxiliary equipment loads under the defined operating conditions. Using the experimentally obtained pressure and temperature values, the total heat transfer rates of key components in the cycle—such as the evaporator, condenser, heat exchanger, and compressor—were also calculated for both refrigerant configurations. A reference commercial vertical deep freezer originally operating with R404A was retrofitted to operate with R290 in order to improve energy efficiency and reduce environmental impact. The thermodynamic performance of both configurations was evaluated through energy and exergy analyses.

In the reference design, there is 305 g of R404A refrigerant. The wire-and-tube condenser located at the rear of the cabinet facilitates heat rejection from the high-pressure refrigerant discharged by the compressor. The throttling process is carried out by a capillary tube with dimensions Ø0.8 × 4000 mm. A finned-tube evaporator is placed on each shelf to ensure uniform cooling performance throughout the cabinet. Temperature regulation is maintained using a mechanical thermostat. Additionally, a radial fan is installed inside the freezer compartment to promote homogeneous air distribution. To enhance heat rejection, another radial fan is positioned beneath the rear-

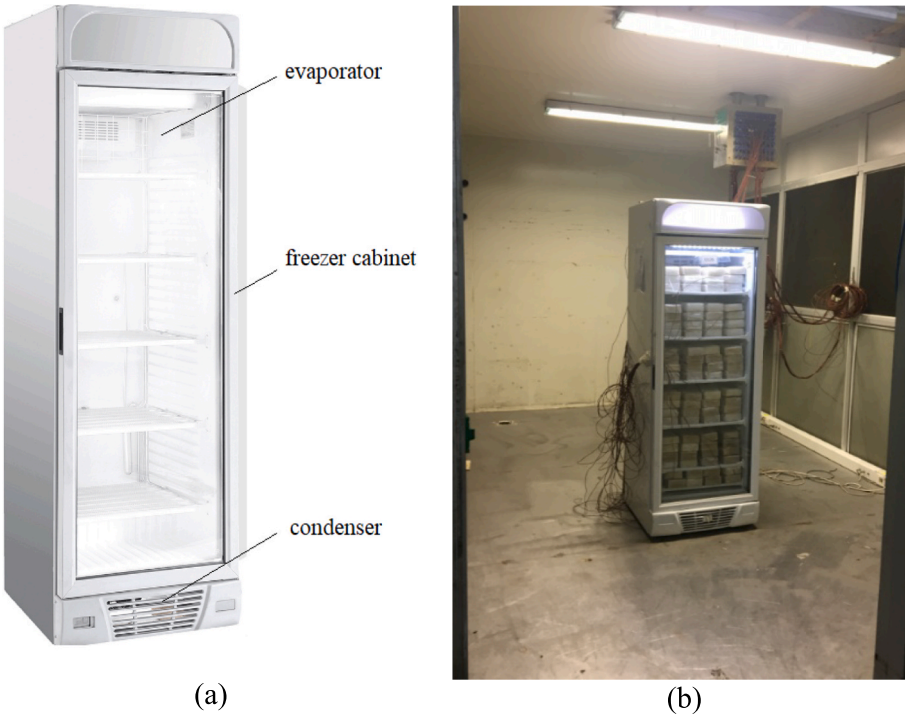

Fig. 1. (a) SCCVDF and (b) the general view of test room.

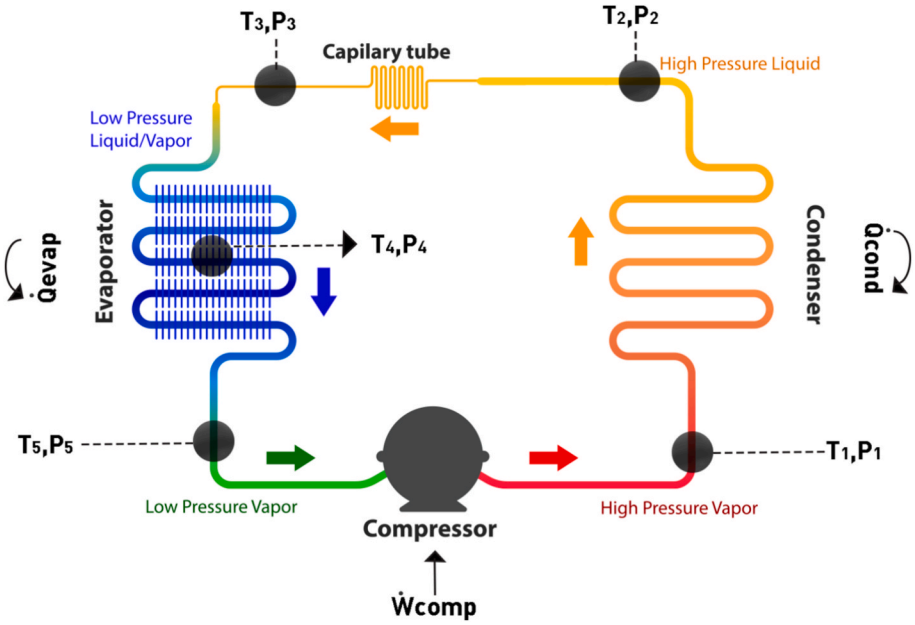

Fig. 2. Vapour compression cycle.

Table 1
The environmental and physical properties of refrigerants [26].

Refrigerant	Classification	Molecular weight (kg/kmol)	T_{CR} (°C)	P_{CR} (MPa)	NBP (°C)	ODP	GWP	Safety class
R404A	HFC	97.6	72.12	3.765	−46.5	0	3921	A1
R290	HC	44.096	134.6	4.23	−42.09	0	11	A3

mounted wire-and-tube condenser. This configuration promotes forced convection, increasing the heat transfer rate from the condenser surface. The resulting rise in enthalpy difference, due to a greater temperature gradient at constant pressure, improves the overall system efficiency by increasing the rejected heat load.

Within the scope of this study, the original compressor (Embraco NEK2150GK) used for the R404A refrigerant was replaced with a propane-compatible model (Embraco NEU2155U) for the R290 configuration, without altering any other system components. The comparative tests were carried out in a climate-controlled chamber in accordance with ISO 23953–2:2012 standards. According to this standard, the ambient air velocity was maintained at approximately 0.25 m/s, while the temperature ranged from 10 °C to 43 °C, with relative humidity levels reaching up to 80 % under specific climate class conditions. The test chamber also has thermal insulation so that it is not affected by the ambient temperature. The temperature, power, current, and pressure values measured over the freezer in the test room are transferred to the computer every 60 s by the data acquisition system, in accordance with the ISO 23953–2:2012 standard, which prescribes recording intervals of 60 s during performance testing.

During the tests, the measurements of the system pressure are recorded by pressure transducers, and temperatures of the freezer and the test packages are occurred by means of OMEGA brand T type thermocouple. To reduce the risk of leakage and pressure losses, the thermocouple tips were not inserted directly into the fluid but were instead attached to the outer surfaces of the copper tubing. This measurement method is widely adopted in both domestic and commercial vertical deep freezer testing practices due to its practicality. Since the pipe walls are thin and thermal conductivity is high, the surface temperature of the pipe closely approximates the internal fluid temperature, making it an acceptable engineering assumption for this type of system.

2.4. Test package

In freezer features, test packages are used to simulate the usage conditions of the consumer and to measure the cooling performance of the freezer. Test packages are available in 1000, 750, 500, and 250 and 125 g weights and in different sizes. Test packages with a freezing point of −1.0 °C contain 23.0 % oxyethylene methyl cellulose methylcellulose, 76.4 % water, 0.5 % sodium chloride, and 0.08 % 6-chloro-m-cresol.

2.5. Test method

The measurements of the system temperatures of the freezer, the indoor temperatures of the freezer, the power and current values consumed, the system pressure values can be examined and comments on the performance of the freezer are accomplished.

During the tests, the standard is taken as a reference [40]. Accommodating the freezer in the test room, loading test packages volume and temperature measurement points of the test packages are carried out according to the directives specified in the mentioned standard. The conditions of the test room and the temperature classes of the test packages are included in the calculation according to this standard. The tests are carried out at 16 °C 80 % RH, 25 °C 55 %RH, 32 °C 65 %RH and 40 °C 75 %RH ambient conditions, taking into account the climate classes of the regions where the freezer is sold. The test packages used in this study are classified under the L1 temperature class, as defined by the EN ISO 23953-2:2012 standard. This classification permits the temperature of the warmest package to rise up to −15 °C during events such as door openings or defrost cycles, while requiring that, under steady-state conditions, all package temperatures return to and remain at −18 °C or below. The climate class of the test chamber and the temperature classification of the test packages, both based on the same standard, are summarized in Table 2 and Table 3, respectively.

Table 2
Test room climate classes.

Test Chamber Climate Class	Dry thermometer temperature (°C)	Relative humidity (%)
0	20	50
1	16	80
8	23.9	55
2	22	65
3	25	60
4	30	55
6	27	70
5	40	40
7	35	75

Table 3
Temperature classes of packages.

Class	Highest Temperature of the Hottest M Package (°C)	Lowest Temperature of the Coldest M Package (°C)	Lowest Temperature of All Packages (°C)
L1	−15	–	−18
L2	−12	–	−18
L3	−12	–	−15
M1	5	−1	–
M2	7	−1	–
H1	10	1	–
H2	10	−1	–
S	Special Classification		

According to the L1 class, a temporary temperature increase up to −15 °C is acceptable during door openings or defrost periods. However, after these events, the package temperatures must decrease to −18 °C and must not exceed this threshold during stable operation. There are no restrictions regarding the minimum temperature the test packages may reach. These classifications are used to evaluate the freezer's performance under various environmental conditions and to ensure that refrigeration equipment complies with international performance standards.

According to the values given in the standard, the temperature class of test packages that are the highest temperature of the hottest M Package, the lowest temperature of the coldest M Package, and the lowest temperature of all Packages are included in the calculation. Test packages with temperature measurements are called M packages. The placement of M packages is crucial for ensuring accurate and consistent testing for several reasons: Accurate Temperature Distribution Measurement; M packages are used to measure temperature variations in different areas of the freezer. Their placement must cover both the coldest and warmest regions of the freezer. This ensures that the temperature distribution is homogeneous throughout the unit.

Impact of door opening, the location of the packages is critical in assessing the effect of door openings on the internal temperature. Packages placed closest to the door help evaluate how quickly the freezer can restore the desired temperature after exposure to warm air. This is particularly important for commercial vertical deep freezers, where the doors are frequently opened. Assessing system performance, temperature readings from different points within the freezer help determine how effectively the cooling system operates. By strategically placing M packages in various locations, the performance of the system across different areas can be measured, providing insights into overall

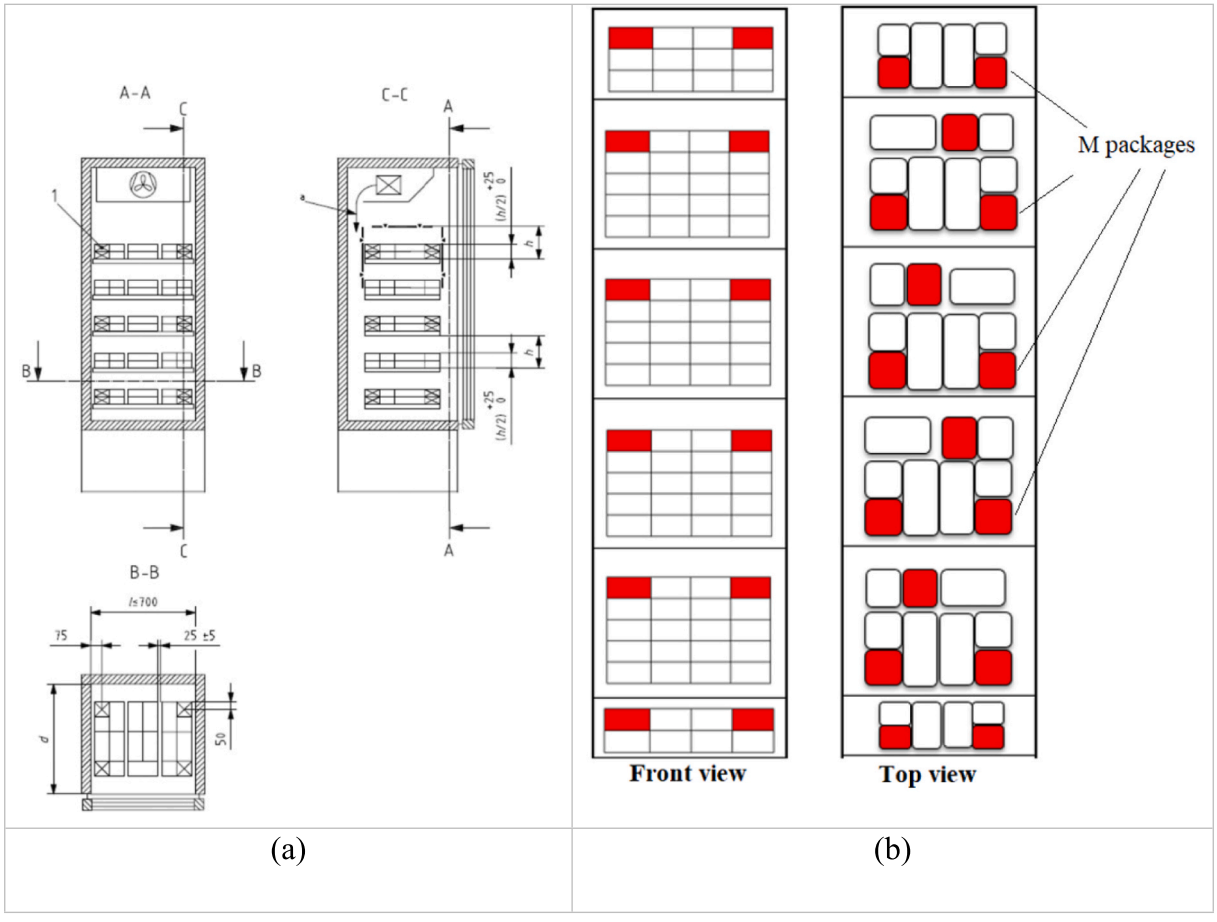

Fig. 3. (a)Deep freezer loading plan in international testing standards (b) Deep freezer loading plan front and top view.

efficiency. And compliance with standards; the placement of M packages must adhere to international testing standards [40]. These standards specify certain locations for the packages to ensure that the results are comparable across different tests and products. For these reasons, the correct placement of M packages is essential for the accuracy of performance tests on freezers. Fig. 3a shows the freezer loading plan in international testing standards [40]. The M packages are placed at the top and front of the rightmost and leftmost package stack on each shelf (Fig. 3b).

In shelf-cooled deep freezers, the cooling efficiency decreases with increasing distance from the evaporator coils. Therefore, the test packages are deliberately placed at the furthest positions from the evaporator and in close proximity to the door gasket, which is one of the regions most prone to heat gain. This placement ensures the monitoring of maximum temperature deviations during door opening/closing cycles and compressor shutdowns, which are critical conditions for product safety assessment.

3. Energy and exergy analysis

The control volume approach is used to perform the energy and exergy analysis of the SCCVDF. For steady-state conditions, energy, the mass, entropy, and exergy balance equations are used to define the heat-work relation, the rate of irreversibility (the other words, exergy destruction rates). A vapour compression cycle is typically used to heat transfer from a low to a high-temperature area. In the evaporator, heat is added to the system and provided to the compressor, while heat rejection occurs from the system in the condenser.

During the analysis,

- The system is assumed as a steady-state, and the flow is taken to a continuous flow.
- The pressure and temperature of the reference is considered as 25 °C and 1 atm.
- Throughout the cycle, the friction losses is neglected in the systems,
- The kinetic −potential energy changes and exergies are negligible,
- Due to the mass balance, the amount of mass at the inlet control volume and the amount of mass at the outlet control volume are equal.

The mass balance equation for the control volume is expressed in Eq. (1).;

$$\sum \dot{m}_{in} = \sum \dot{m}_{out} \tag{1}$$

The energy balance for the system is written as in Eq. (2);

$$\dot{E}_{in} - \dot{E}_{out} + \dot{E}_{generation} = \Delta E \tag{2}$$

Assuming the changes in kinetic and potential energy and exergies are negligible, the energy balance equation is written as shown in Eq. (3);

$$\dot{Q} - \dot{W} = \sum \dot{m}_{out} h_{out} - \sum \dot{m}_{in} h_{in} \tag{3}$$

The energy efficiency can be written as shown in Eq. (4);

$$\varepsilon = \frac{\dot{E}_{out}}{\dot{E}_{in}} \tag{4}$$

The entropy generation is written using the entropy balance equation, as shown in Eq. (5). [42];

$$\dot{S}_{gen} = \sum (\dot{m}s)_{out} - \sum (\dot{m}s)_{in} - \sum \frac{\dot{Q}}{T} \tag{5}$$

Using the flow exergy or specific exergy as given in Eq. (6) [42]

$$\psi = [(h - h_0) - T_0(s - s_0)] \tag{6}$$

Exergy destruction rates can be identified using Eq. (7).;

$$Ex_{dest} = T_0 \dot{S}_{gen} \tag{7}$$

The exergy efficiency is calculated using Eq. (8);

$$\eta = \frac{\sum \dot{E}x_{out}}{\sum \dot{E}x_{in}} = 1 - \frac{\sum \dot{E}x_{dest}}{\sum \dot{E}x_{in}} \tag{8}$$

In the ideal refrigeration cycle, the compression operating in the compressor is internally adiabatic and reversible. However, losses from flow friction and heat transfer occur during the actual compression process.

In this study, the transfer of the heat released in the friction source compressor to the environment is taken into account. For a reversible system, exergy can be conserved. All real processes are irreversible and irreversibility related to these processes causes exergy destruction [43]. The exergy balance in a steady state for a control volume is given by Eq. (9). [44–46];

$$\dot{E}x_{dest} = \sum \dot{E}x_{in} - \sum \dot{E}x_{out} + \sum \left[\dot{Q}\left(1 - \frac{T_0}{T}\right)\right]_{in} - \sum \left[\dot{Q}\left(1 - \frac{T_0}{T}\right)\right]_{out} + \sum \dot{W}_{in} - \sum \dot{W}_{out} \tag{9}$$

The total exergy destruction is shown in Eq. (10),

$$\dot{E}x_{dest,T} = \dot{E}x_{\mathrm{dest,cond}} + \dot{E}x_{dest,cap} + \dot{E}x_{dest,comp} + \dot{E}x_{dest,evap} \tag{10}$$

Exergy balances for each part of the refrigeration cycle are applied to calculate energy and mass balances in addition to exergy destructions. For the system, the exergy efficiency is defined in Eq. (11) [43]

$$\eta = \frac{S\dot{E}x_{out}}{S\dot{E}x_{in}} = 1 - \frac{S\dot{E}x_{dest}}{S\dot{E}x_{in}} \tag{11}$$

The energy efficiencies of the SCCVDF is calculated as the ratio of heat transfer rate for evaporator to net power as shown in Eq. (12).

$$COP = \frac{\dot{Q}_{evap}}{\dot{W}_{net}} \tag{12}$$

In the exergy analysis of the system components, exergy balance equations were formulated to quantify irreversibilities. These equations reflect the actual performance losses occurring in each component due to thermodynamic inefficiencies. For each major component, the following exergy balance relations were applied: In the vapor-compression cycle of the deep freezer, Points 1 to 5 represent the key thermodynamic states of the refrigerant. Point 1 is the compressor outlet and condenser inlet (high-pressure superheated vapor), and Point 2 is the condenser outlet (high-pressure liquid). After expansion through the capillary tube, Point 3 represents a low-pressure, low-temperature mixture. The refrigerant then enters the evaporator. Point 4 is the midpoint of the evaporator, used for average property calculations. Finally, Point 5 is the evaporator outlet and compressor inlet (low-pressure vapor). These state points are essential for energy and exergy analysis of the deep freezer system.

Eq. (13) accounts for the exergy reduction associated with heat rejection and internal losses in the condenser.

$$\dot{m}\,Ex_1 - \dot{m}\,Ex_2 - \dot{E}x_{,\mathrm{loss}} - \dot{E}x_{,Q_H} = 0 \tag{13}$$

As a throttling device, the capillary tube introduces an irreversible pressure drop and exergy destruction without performing work as in Eq. (14);

$$\dot{m}\,Ex_2 - \dot{m}\,Ex_3 - \dot{E}x_{,\mathrm{loss}} = 0 \tag{14}$$

This expression evaluates the gain in exergy due to heat absorption

and the internal losses associated with the evaporation process (Eq (15).

$$\dot{m}\,Ex_3 - \dot{m}\,Ex_5 - \dot{E}x_{,loss} + \dot{E}_{x,}Q_L = 0 \quad (15)$$

The exergy equation of the compressor reflects the conversion of input work into pressure and temperature rise, considering associated losses due to non-ideal compression (Eq (16).

$$\dot{m}\,Ex_3 - \dot{m}\,Ex_5 - \dot{E}x_{,loss} + \dot{E}_{x,}Q_L = 0 \quad (16)$$

While the exergy efficiency and exergy performance indicators confirm the superior thermodynamic behavior of the R290 system, the thermodynamic model adopted in this study is based on steady-state assumptions. Transient effects such as compressor cycling, load fluctuations, or door openings—which frequently occur in real commercial refrigeration environments—are not included in the analysis. Additionally, the compression process is modeled with a fixed isentropic efficiency derived from manufacturer data, assuming idealized performance under constant operating conditions. While this approach provides a consistent basis for comparative evaluation, it may not fully capture variations in compressor behavior under off-design or part-load conditions.

4. Results and discussions

4.1. Experimental measurement

In this study, R404A refrigerant is replaced with R290 refrigerant in a SCCVDFs are investigated. Energy and exergy analyzes are carried out using the experimental measurements obtained from the test setup, and as a result of the energy and exergy analyzes, the losses of exergy of the components and the energy and exergy efficiencies of whole system are compared. The experimental measurement values obtained from the test setup in the environment conditioned at 25 °C in the test room are given in Table 1 for R404A and R290 refrigerants. It is observed that the system with R404A refrigerant works at a higher pressure on the high pressure side than the system with R290 refrigerant. Lower temperatures are observed at the same temperature measurement points in the system with R404A. The work consumed by the compressor of the system with R404A and R290 refrigerants are 0.508 kW, 0.510 kW, respectively. Table 4 shows that the power consumption of the R404A and R290 compressors are nearly identical (0.508 kW vs. 0.510 kW). Despite this, the R290 system achieves an 8 % higher cooling capacity, demonstrating better energy conversion efficiency, consistent with previous findings by Saraç and Ünaldı [20] and Polukhin and Yakovleva [22], who also reported significant COP improvements with R290 in commercial systems.

In Table 5, the minimum, maximum and average temperatures of all M packages of the system with R404A and R290 refrigerant are given. According to the ISO 23953–2:2005 + A1:2012 test standard [40], the maximum temperature of the test packs should not exceed −18 °C under normal operating conditions. The temperature measurement values provided comply with the standard [40] for the freezer.

Table 4
Freezer system temperatures of the R404A and R290 refrigerants at 25 °C.

System Measurement Points		R404A Refrigerant System	R290 Refrigerant System
Compressor Outlet-Point 1	(°C)	80.0	83.5
Condenser outlet-Point 2	(°C)	30.1	39.5
Evaporator inlet- Point 3	(°C)	−34.9	−29.9
Midpoint of Evaporator –Point 4	(°C)	−34.6	−30.5
Evaporator outlet-Point 5	(°C)	−21.9	−19.9
High Pressure	bar	19.8	14.5
Low Pressure	bar	2.0	1.7
Power	kW	0.508	0.510

Table 5
M package temperatures of the R404A and R290 refrigerants at 25 °C.

M Package Temperatures		R404A Refrigerant System	R290 Refrigerant System
Minimum temperature of packages	(°C)	−22.8	−21.6
Maximum temperature of packages	(°C)	−18.0	−18.2
Average temperature of packages	(°C)	−21.2	−20.0

4.2. Energy and exergy analysis results

The heat and power interactions (energy analysis) of the investigated systems are given in Table 6. Against the 0.508 kW power consumed by the compressor, 0.734 kW of heat is extracted from the freezer interior. When the actualized condenser heat transfer rates of both systems are compared, it is observed that the system using R404A refrigerant dissipates 666 W of heat, while the R290 refrigerant system achieves 0.743 kW of heat dissipation. Under identical conditions and using the same condenser, the R290 system achieves a higher heat transfer rate, indicating improved thermal performance compared to the R404A system. Considering that the energy consumption of both systems is almost the same, this is an indication that the system with R290 increases the cooling capacity. In the system with R404A refrigerant, 0.327 kW heat loss occurs in the capillary tube, while this loss is 0.330 kW in the system with R290 refrigerant. Heat loss in the compressor occurs due to the heating occurring in the compressor during the compression of the refrigerant. In the system with R404A refrigerant, 249 W heat loss occurs during compression, while it is determined as 0.230 kW in the system with R290 refrigerant.

For the system using R404A refrigerant, 54 % of the total input energy is rejected as heat in the condenser, while 26 % flows into the capillary tube, and 20 % is lost as heat dissipation from the compressor. In comparison, the R290 system rejects 57 % of the total input energy as heat in the condenser, improving overall heat transfer efficiency. Apart from this, 25 % of the total energy in the R290 system enters the capillary tube, and 18 % is dissipated in other components. As illustrated in Fig. 4, the compressor is the dominant source of exergy loss, accounting for 83 % in the R290 system and 78 % in the R404A system. This confirms that compressor inefficiencies significantly impact overall system performance.

Exergy analysis indicates that the compressor is responsible for the highest exergy destruction in both systems. The compressor accounts for 80.46 % of the total exergy destruction in the R290 system and 78.16 % in the R404A system.

However, due to the improved thermodynamic properties of R290, compressor exergy losses are reduced by 26 % compared to R404A. This reduction allows more input energy to be effectively converted into useful cooling, leading to lower power consumption and enhanced system sustainability. Additionally, the evaporator causes greater exergy destruction than the condenser, indicating that minimizing energy losses in the evaporator could further improve system performance.

Component-wise percentage distribution of exergy losses in the R290 Refrigerant System in Fig. 4(a) and in the 404A Refrigerant System

Table 6
Energy analysis of the systems with R404A and R290 refrigerant.

Equipment	system with R404A refrigerant (kW)	system with R290 refrigerant (kW)
$\dot{W}_{comp}$	0.508	0.510
$\dot{Q}_{evap}$	0.734	0.793
$\dot{Q}_{comp}$	0.249	0.230
$\dot{Q}_{cap}$	0.327	0.330
$\dot{Q}_{cond}$	0.666	0.743

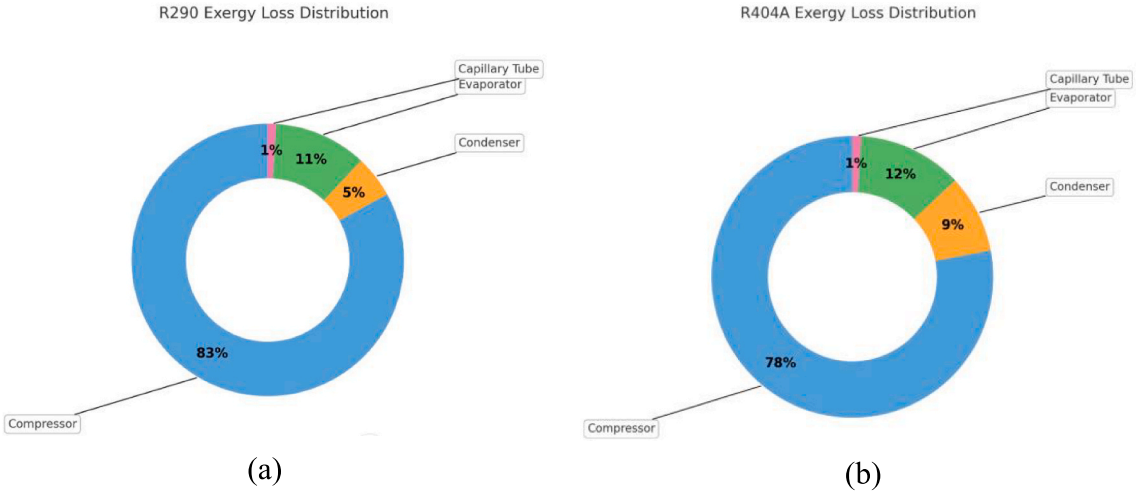

Fig. 4. Component-wise percentage distribution of exergy losses (a) in the R290 refrigerant system (b) in the 404A Refrigerant System.

shown in Fig. 4(b). The loss of exergy caused by the compressor is 0.297 kW in the system with R404A refrigerant and 0.282 kW in the system with R290 refrigerant. The system with R404A refrigerant exhibited higher exergy losses than the R290-based system across all components. In both cases, the compressor was identified as the dominant source of exergy destruction, primarily due to higher irreversibilities arising from mechanical processes. This observation aligns with earlier studies that identified the compressor as the major contributor to exergy destruction in vapor-compression cycles, particularly in systems retrofitted with hydrocarbon refrigerants such as R290 [24].

Comparing the exergy losses in the condenser it is seen that the exergy loss in the system with R404A refrigerant is more than twice the exergy loss in the system with R290 refrigerant. Exergy losses of components in systems with R404A and R290 refrigerant are shown in Fig. 5.

When the exergy losses of the systems are examined, it is observed that the R404A based system causes a total of 0.043 kW more exergy loss compared to the R290 based system. Considering that exergy represents the useful work potential within the system, this indicates that the R404A cycle experiences a greater loss of useful energy. The reduction of total exergy losses not only enhances thermodynamic efficiency but also contributes to system sustainability, in line with the objectives of exergy-focused evaluations proposed by Dincer and Rosen [43].

In Fig. 6, COPs and exergy efficiencies of systems for R404A and R290 refrigerants are shown comparatively.

The exergy efficiency of the system with R404A refrigerant and system with R290 are 0.24 and 0.28, respectively. The exergy losses in the compressor for both systems are given as a comparison of the exergy and energy efficiencies of the compressor. The energy efficiency of the compressor used in the system with R290 refrigerant is 0.55, and the energy efficiency value of the compressor of the system with R404A refrigerant is 0.51. The compressor of the system with R290 refrigerant caused lower exergy loss than the compressor of the system with R404A refrigerant.

Exergy losses, Exergy efficiency and Exergy losses in compressors of system with R290 and R404A refrigerant are shown in Fig. 7. According to this figure, the exergy loss in the R404A-based system is 0.297 kW, whereas it is 0.2189 W in the R290-based system. When the energy efficiencies of the compressors are compared, the compressor used in the R290 system exhibits an energy efficiency of 0.55, while the corresponding value for the R404A system is calculated as 0.51. Based on Fig. 7, the exergy efficiency of the R404A system is 0.3665, whereas the exergy efficiency of the R290 system is 0.4083. This corresponds to an approximately 17 % improvement in exergy efficiency when using R290, indicating enhanced utilization of available energy in the compression process. Similar improvements in exergy efficiency with R290 have also been reported in earlier comparative studies involving hydrocarbon refrigerants in vapor-compression systems [24].

The compressor operating with R290 results in a lower exergy loss

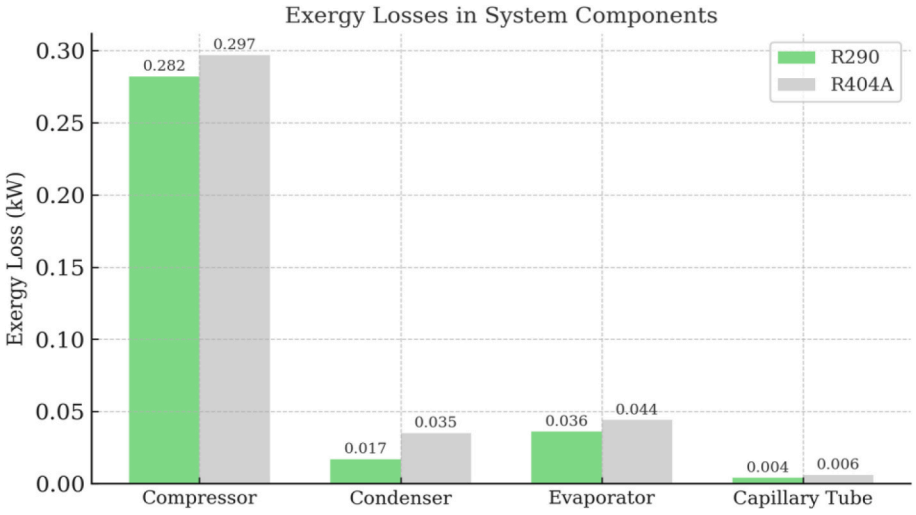

Fig. 5. Exergy losses of components in systems with R404A and R290 refrigerant.

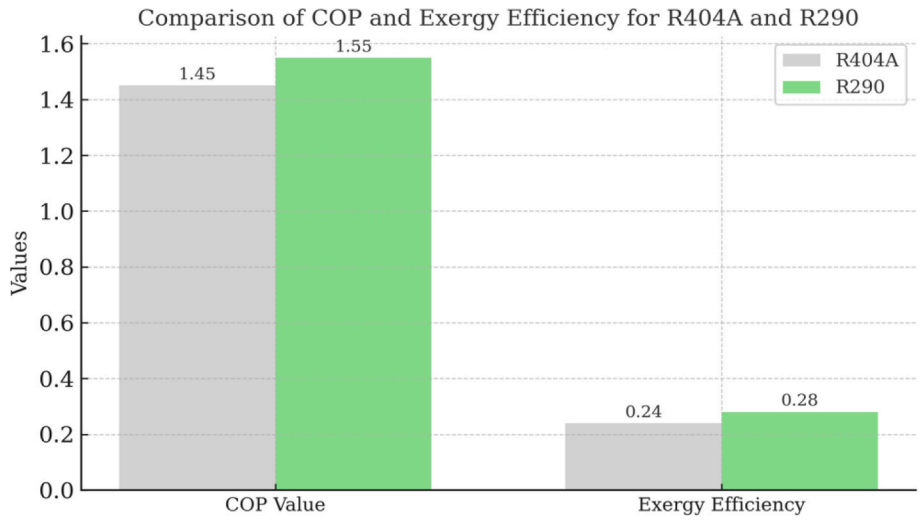

Fig. 6. Comparison of COP values and exergy efficiency for refrigerant.

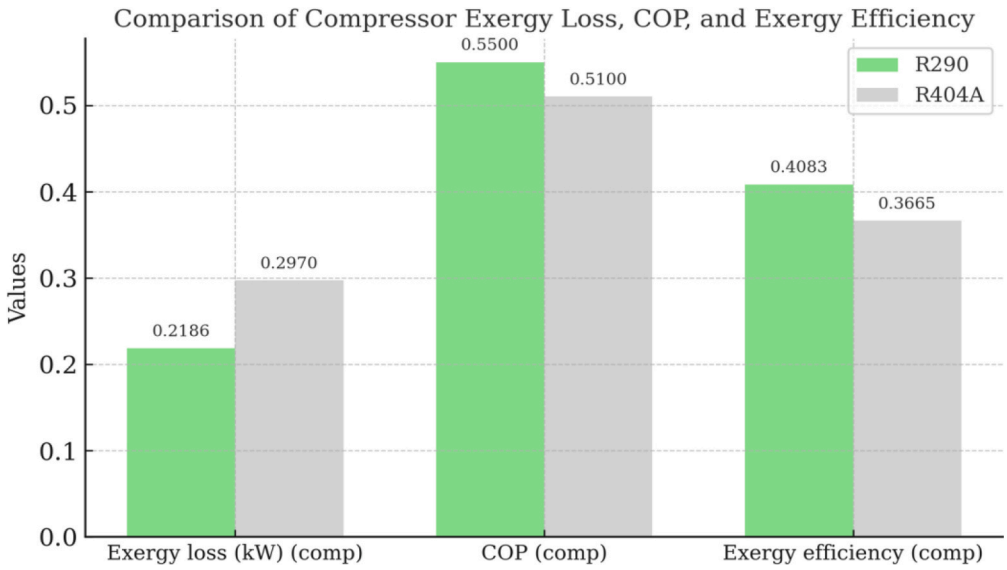

Fig. 7. Exergy losses, COP and exergy efficiency in compressors of system with R290 and R404A refrigerant.

than the one operating with R404A. This outcome demonstrates that the compressor in the R290 system performs better in terms of both energy and exergy efficiency. As mentioned, the highest exergy loss in both systems occurs in the compressor. Therefore, reducing the exergy loss in the compressor is critical for improving overall system performance.

The experimental results revealed that the cooling capacity of the R290-based system was measured at 0.793 kW, which corresponds to an 8.0 % improvement compared to the R404A-based system, which achieved 0.734 kW under identical test conditions. Furthermore, the compressor power consumption of the R290 system was slightly lower, recorded at 0.377 kW versus 0.392 kW for the R404A system, representing a 3.8 % reduction in energy usage (Table 7). As a result of the increased cooling output and reduced energy input, the COP improved from 1.87 (R404A) to 2.00 (R290), corresponding to a 7.0 % enhancement in energy efficiency.

These findings confirm that the R290 retrofit not only improves system performance in terms of cooling capacity but also reduces power consumption, thereby enhancing overall energy efficiency. Due to this situation, the compressor of the system using R290 refrigerant performs with more exergy and energy efficiency than the compressor of the system using R404A refrigerant. As stated before, the highest exergy loss occurs in the compressor in both systems. Therefore, the reduction in the loss of exergy of the compressor is significant in terms of improving the performance of the system. Exergy analysis aims to determine the system's maximum performance and to identify a solution for exergy destruction [47].

Table 7
Experimental Comparison of Cooling Capacity, Power Consumption, and COP between R404A and R290.

Parameter	R404A System	R290 System	Improvement (%)
Cooling Capacity (kW)	0.734	0.793	+8.0 %
Compressor Power (kW)	0.392	0.377	−3.8 %
COP	1.87	2.00	+7.0 %

4.3. Measurement devices and accuracy

The experimental investigation was performed on a shelf-cooled commercial vertical deep freezer, originally operating with R404A refrigerant. To assess the applicability of R290 as a replacement, the system was retrofitted by replacing only the compressor, while keeping

the evaporator, condenser, and capillary tube unaltered. This ensured that all thermal and structural boundary conditions remained consistent between the two configurations.

The experiments were conducted in a climate-controlled laboratory environment following ISO 23953–2:2012 standards. During the tests, the ambient temperature was maintained at 25 ± 0.5 °C, and the relative humidity did not exceed 60 %. The airflow velocity surrounding the cabinet was held at 0.25 m/s, simulating typical commercial operating conditions. All temperature measurements were recorded at 60-second intervals using calibrated sensors.

To ensure precise monitoring of system performance, calibrated instruments with known accuracies were employed throughout the experiments. Temperature measurements were carried out using Type-K thermocouples with an accuracy of ±0.5 °C. These were externally affixed to the copper piping using thermal paste and insulated to minimize heat loss and external interference. Pressure readings at the compressor's suction and discharge lines were obtained using Bourdon-type mechanical pressure gauges with an accuracy of ±0.25 bar. Compressor power consumption was measured using a digital wattmeter with ±1 % accuracy. Finally, the amount of refrigerant charge in each configuration was determined with a high-precision digital scale offering a resolution of 1 g.

4.4. Uncertainty analysis

To evaluate the accuracy and reproducibility of the measurements, an uncertainty analysis was performed using the root-sum-square (RSS) method, which accounts for the propagation of uncertainties originating from temperature, pressure, and power measurements into the derived performance indicators. Based on this approach, the estimated uncertainty in the calculation of cooling capacity was ±2.4 %, while the uncertainty in COP was determined to be ±3.1 %. Each test was repeated three times for both refrigerant configurations, and the average values were used in performance assessments. These methodological steps ensure the robustness of the experimental setup and confirm the reliability of the reported results.

5. Conclusion

This experimental study evaluated and compared the thermodynamic performance of a shelf-cooled commercial vertical deep freezer using R404A and R290 (propane) under identical operating conditions. All system components remained unchanged except for the compressor, which was replaced with a compatible model for each refrigerant to ensure a fair comparison. The results consistently demonstrated that the R290-charged system outperformed the R404A baseline in all key metrics. Specifically, R290 provided approximately 8 % higher cooling capacity and a 7 % improvement in coefficient of performance, indicating more effective heat extraction and better energy utilization. These advantages were achieved without any structural modifications to the freezer unit beyond the compressor replacement.

Exergy-based analysis further highlighted R290′s superior thermodynamic behavior. The R290 system exhibited a 17 % higher exergy efficiency compared to R404A, reflecting significantly reduced irreversibilities throughout the cycle. The total exergy losses in the R290 system were approximately 0.043 kW lower, indicating a notable reduction in useful work loss across the cycle. This improvement was primarily influenced by enhanced compressor performance, as the compressor remained the dominant source of exergy destruction in both systems. Additionally, the R290 system maintained more stable operation, characterized by consistent evaporator outlet temperatures throughout the test duration.

From an environmental perspective, transitioning from R404A to R290 led to a near-complete elimination of direct greenhouse gas emissions. Due to R290′s negligible Global Warming Potential (approximately 3) and zero ozone depletion potential, the system's equivalent CO_2 emissions were reduced by roughly 99.92 %. This aligns the technology with global climate goals and current regulatory mandates, such as those set by the European Union's F-Gas regulation.

In summary, R290 proves to be a viable and highly effective replacement for R404A in shelf-cooled commercial freezer systems. It offers better thermal and exergetic performance, enhanced operational consistency, and an exceptionally low environmental footprint—all without requiring major design changes. Future studies should expand upon these findings by testing low-impact refrigerants like R290 under varying ambient conditions and system configurations. Comparative evaluations with other eco-friendly alternatives are also recommended to identify optimal refrigerant solutions for broader commercial applications.

CRediT authorship contribution statement

Egemen Biçen: Writing – original draft, Validation, Resources, Methodology, Investigation. **Seda Kırmacı Arabacı:** Writing – review & editing, Validation, Supervision, Methodology, Investigation.

Declaration of competing interest

The authors declare that they have no known competing financial interests or personal relationships that could have appeared to influence the work reported in this paper.

Acknowledgements

This work was supported by Klimasan of Turkey. The authors are indebted to Efmas Engineering.

Data availability

Data will be made available on request.

References

[1] N. Abas, A.R. Kalair, N. Khan, A. Haider, Z. Saleem, M.S. Saleem, Natural and synthetic refrigerants, global warming: a review, Renew. Sustain. Energy Rev. 90 (2018) 557–569.
[2] I.C. Change, Climate Change: The Physical Science Basis, Cambridge University Press, 2013.
[3] M. Mohanraj, S. Jayaraj, C. Muraleedharan, Environment friendly alternatives to halogenated refrigerants–a review, Int. J. Greenh. Gas Con. 3 (2009) 108–119.
[4] E. Granryd, Hydrocarbons as refrigerants–an overview, Int. J. Refrig. 24 (2001) 15–24.
[5] B.O. Bolaji, Z. Huan, Ozone depletion and global warming: case for the use of natural refrigerant – a review, Renew. Sustain. Energy Rev. 18 (2013) 49–54.
[6] J.M. Calm, Refrigerant transitions again moving towards sustainability. In: Proceedings of the ASHRAreferasnE/NIST conference. Gaithersburg, MD, USA, 2010.
[7] B. Palm, Refrigeration systems with minimum charge of refrigerant, Appl. Therm. Eng. 27 (2007) 1693–1701.
[8] F. Poggi, H. Macchi-Tejeda, D. Leducq, A. Bontemps, Refrigerant charge in refrigerating systems and strategies of charge reduction, Int. J. Refrig. 31 (2008) 353–370.
[9] K.S. Kumar, K. Rajagopal, Computational and experimental investigation of low ODP and low GWP HCFC-123 and HC-290 refrigerant mixture alternate to CFC12, Energ. Conver. Manage. 48 (2007) 3053–3062.
[10] B.O. Bolaji, Z. Huan, Ozone depletion and global warming: Case for the use of natural refrigerant–a review, Renew. Sustain. Energy Rev. 18 (2013) 49–54.
[11] J.M. Belman-Flores, R. Román-Aguilar, J. Valle-Hernández, J. Serrano-Arellano, Theoretical investigation of low global warming potential blends replacing R404A: the simple refrigeration cycle and its modifications, J. Therm. Sci. Eng. Appl. 16 (4) (2024).
[12] Regulation (EU) No 517/2014 of the European Parliament and the Council of 16 April (2014) on fluorinated greenhouse gases and repealing Regulation (EC) No 842/2006. Off. J. Eur. Union, 2014.
[13] F. Gonçalves, M. Cavique, F-Gas regulation-Possible solutions for the retrofit dead end. In MATEC Web of Conferences, EDP Sciences, 178 (2018) 09023.
[14] T. Kivevele, Propane (HC–290) as an alternative refrigerant in the food transport refrigeration sector in Southern Africa–a review, 2022. doi: 10.31603/ae.5994.
[15] C. Camponeschi, M. Goni, F. Cioffi, M. Dongellini, C. Naldi, G.L. Morini, L. Ballotta, Potential of Energy Saving of Propane Heat Pump as replacement of gas boilers

with low and high temperature emitters. In E3S Web of Conferences (Vol. 523, p. 03004). EDP Sciences, 2024, doi: 10.1051/e3sconf/202452303004.
[16] H. Tan, M. Bai, L. Xu, X. Li, Z. Liu, Experimental study on the pull-down performance of a− 80° C cascade refrigeration freezer, Asia Pac. J. Chem. Eng. 18 (3) (2023) e2888.
[17] E. Halimic, D. Ross, B. Agnew, A. Anderson, I. Potts, A comparison of the operating performance of alternative refrigerants, Appl. Therm. Eng. 23 (12) (2003) 1441–1451.
[18] M.A. Kedzierski, Enhancement of R123 pool boiling by the addition of hydrocarbons, Int. J. Refrig. 23 (2) (2000) 89–100.
[19] D. Jung, C.B. Kim, K. Song, B. Park, Testing of propane/isobutane mixture in domestic refrigerators, Int. J. Refrig. 23 (2000) 517–527.
[20] T. Saraç, M. Ünaldı, R290 Refrigerant Performance in a Commercial Refrigerator, J. Faculty Eng., Çukurova University 39 (1) (2024) 157–166, https://doi.org/10.21605/cukurovaumfd.1459421.
[21] O. Pektezel, M. Das, H. Ibrahim Acar, Experimental analysis of different refrigerants' thermal behavior and predicting their performance parameters, J. Thermophys. Heat Transfer 37 (2) (2023) 309–319, https://doi.org/10.2514/1.t6660.
[22] V. Polukhin, O. Yakovleva, Analysis of refrigerants used in supermarket commercial equipment and the potential for increasing energy efficiency and reducing environmental impact, Technology Audit and Production Reserves 3 (3 (77)) (2024) 30–35.
[23] A. Sethi, G. Pottker, S. Yana Motta, Experimental evaluation and field trial of low global warming potential R404A replacements for commercial refrigeration, Sci. Technol. Built Environ. 22 (8) (2016) 1175–1184, https://doi.org/10.1080/23744731.2016.1209032.
[24] T.B. Fajar, P.R. Bagas, S. Ukhi, M.I. Alhamid, A. Lubis, Energy and exergy analysis of an R410A small vapor compression system retrofitted with R290, Case Stud. Therm. Eng. 21 (2020) 100671.
[25] M. Koşan, Investigation of using low GWP alternatives to replace R404A in the refrigeration system, Int. J. Energy Studies 8 (3) (2023) 453–464, https://doi.org/10.58559/ijes.1335092.
[26] E. Mancuhan, A comprehensive comparison between low and medium temperature application refrigerants at a two-stage refrigeration system with flash intercooling, Therm. Sci. Eng. Progr. 13 (2019) 100357, https://doi.org/10.1016/j.tsep.2019.100357.
[27] M. Vaughn, 2022-2023 ASHRAE Research Report, ASHRAE J. 65 (10) (2023).
[28] M.W. Spatz, S.F.Y. Motta, An evaluation of options for replacing HCFC-22 in medium temperature refrigeration systems, Int. J. Refrig. 27 (2004) 475–483.
[29] J.M. Corberan, I.O. Martinez, J. Gonzalves, Charge optimization study of a reversible water-to-water propane heat pump, Int. J. Refrig. 31 (2008) 716–726.
[30] P. Fernando, B. Palm, P. Lundqvist, E. Granryd, Propane heat pump with low refrigerant charge: design and laboratory tests, Int. J. Refrig. 27 (2004) 761–773.
[31] A. Cavallini, E. Da Riva, D. Del Col, Performance of a large capacity propane heat pump with low charge heat exchangers, Int. J. Refrig. 33 (2010) 242–250.
[32] J.U. Ahamed, R. Saidur, H.H. Masjuki, A review on exergy analysis of vapor compression refrigeration system, Renew. Sustain. Energy Rev. 15 (3) (2011) 1593–1600, https://doi.org/10.1016/j.rser.2010.11.039.
[33] S. Sevim, A. Yurddaş, Energy and exergy analysis of the heating and cooling system of a public building, Int. J. Exergy 32 (2) (2020) 186–212, https://doi.org/10.1504/IJEX.2020.108181.
[34] M. Xing, H. Zhang, C. Zhang, An update review on performance enhancement of refrigeration systems using nano-fluids, J. Therm. Sci. 31 (4) (2022) 1236–1251, https://doi.org/10.1007/s11630-022-1607-8.
[35] H. Demirpolat, S. Erten, Ş. Ataş, M. Aktaş, M. Özkaymak, Comparison of the impact of R449-A and R290 on refrigerated display cabinets using life-cycle climate performance method, Eur. Mech. Sci. 8 (3) (2024) 125–136, https://doi.org/10.26701/ems.1493164.
[36] I. Dincer, M.A. Rosen, Exergy Analysis of Heating, Refrigerating And Air Conditioning: Methods and Applications, Academic Press, 2015.
[37] R.A. Gaggioli, Available energy and exergy, Int. J. Appl. Thermodyn. 1 (1998) 1–8.
[38] C. Camponeschi, M., Goni F. Cioffi, M. Dongellini, C. Naldi, G.L. Morini, L. Ballotta, Potential of Energy Saving of Propane Heat Pump as replacement of gas boilers with low and high temperature emitters. In E3S Web of Conferences, Vol. 523, p. 03004) (2024). EDP Sciences. doi: 10.1051/e3sconf/202452303004.
[39] R.I.T.A. Mastrullo, A.W. Mauro, L. Menna, G.P. Vanoli, Replacement of R404A with propane in a light commercial vertical freezer: A parametric study of performances for different system architectures, Energ. Conver. Manage. 82 (2014) 54–60.
[40] BS EN ISO 23953-2:2005+A1:2012, Refrigerated display cabinets, Classification, requirements and test conditions, 2012.
[41] T. Venegas, M. Qu, L. Wang, X. Liu, K. Gluesenkamp, Z. Gao, Review of liquid desiccant air dehumidification systems coupled with heat pump: System configurations, component design, and performance, Energ. Buildings 279 (2023) 112655.
[42] T.J. Kotas, Teaching The Exergy Method To Engineers, in: Teaching Thermodynamics, Springer, US, Boston, MA, 1985, pp. 373–385.
[43] I. Dincer, M.A. Rosen, Exergy Analysis of Heating, Refrigerating and Air Conditioning: Methods and Applications, Academic Press, 2015.
[44] M.M. Joybari, M.S. Hatamipour, A. Rahimi, F.G. Modarres, Exergy analysis and optimization of R600a as a replacement of R134a in a domestic refrigerator system, Int. J. Refrig. 36 (4) (2013) 1233–1242, https://doi.org/10.1016/j.ijrefrig.2013.02.012.
[45] H.C. Bayrakçi, A.E. Özgür, Energy and exergy analysis of vapor compression refrigeration system using pure hydrocarbon refrigerants, Int. J. Energy Res. 33 (12) (2009) 1070, https://doi.org/10.1002/er.1538.
[46] A. Hepbasli, Thermoeconomic analysis of household refrigerators, Int. J. Energy Res. 31 (10) (2007) 947–959, https://doi.org/10.1002/er.1290.
[47] R. Saidur, J.U. Ahamed, H.H. Masjuki, Energy, exergy and economic analysis of industrial boilers, Energy Policy 38 (5) (2010) 2188–2197, https://doi.org/10.1016/j.enpol.2009.11.087.